Model for Flue-Gas Desulfurization in a Circulating Dry Scrubber

James K. Neathery
Center for Applied Energy Research, University of Kentucky, Lexington, KY 40511

A simple model was developed to describe the absorption of SO_2 in a circulating dry scrubbing (CDS) process, which is a semidry, lime-based, flue-gas desulfurization (FGD) process that utilizes a circulating fluidized bed arrangement for contacting a sorbent with SO_2-laden flue gas under "coolside" conditions. The reaction chemistry is thought to be similar to that of spray-drying absorption. The liquid-phase mass-transfer coefficient was successfully modeled as a function of the sorbent particle spacing on the wetted surfaces. Gas-phase mass-transfer resistances were assumed to be insignificant. Due to the high surface area available in a CDS reactor, the evaporation rate of water from the slurry was modeled as "constant-rate" drying according to classic spray-dryer theory. However, the "falling-rate" and "diffusion" evaporation stages were negligible in CDS since sorbent particle bunching at the surface of the slurry is nonexistent.

Introduction

Wet flue-gas desulfurization (FGD) processes were the first SO_x control systems to be developed on a commercial scale in the United States. These systems were initially plagued by reliability problems due to a combination of the early status of development at the time, poor design, and questionable operating procedures. In addition, most electric utility plant operators had no previous experience with "chemical plant" operation. By the late 1980s, most of these problems were overcome and some technological advances were made in the scrubbing area that improved wet FGD reliability. However, wet FGD systems remain costly to operate due to large work force requirements, the generation of large quantities of solid waste by-products that must be disposed, and high parasitic energy requirements.

Wet scrubber systems are characterized by high liquid-to-gas ratios (L/G) of liquid sorbent slurry to flue gas. The L/G ratios, ranging from 5,400 to 13,400 l Nm^{-3} (40 to 100 gal/std. kft^3), are high enough to completely saturate the treated flue gas with water vapor. Typically, some untreated flue gas is bypassed around the scrubber modules to reheat the scrubbed gas and prevent troublesome condensation in the duct and stack.

Because of the many shortcomings with wet FGD systems, the power utility industry is continually seeking new processes that will lower the capital, operating, and disposal costs associated with these conventional SO_x control systems. In the early 1980s, pilot studies of semidry FGD processes, such as spray-drying absorption, were conducted to determine their potential as SO_2 control technologies. Many semidry FGD technologies have reached commercial scale in the last decade. As a result, a large number of studies have been performed to research and further develop these processes.

As a contrast to wet FGD systems, semidry systems operate with low L/G ratios (about 28 to 40 l Nm^{-3} or 0.2 to 0.3 gal/std. kft^3) as compared to 5,400 to 13,400 l Nm^{-3} or 40 to 100 gal/kSCF or higher for wet FGD systems). Since massive slurry pipe circuits and the associated pumps are not required, the footprint of semidry systems is usually smaller than that of the bulkier wet FGD systems. As a result, semidry FGD is more readily used in retrofit applications to older power plants.

Like wet FGD systems, spray-dryer processes are designed to treat flue gas downstream of the furnace air preheater (inlet flue-gas temperatures ranging from 138 to 160°C); this area of the furnace system is commonly called the "coolside" of the air preheater. A 20 to 30 wt. % slurry is atomized in a reaction vessel or a portion of the duct large enough to permit a 5 to 12 s flue-gas residence time (Kohl and Riesenfeld, 1985). Slurry atomization is usually effected by a spinning atomizer disk or an aerated, two-fluid (gas–liquid) nozzle. Additional water is added to the slurry stream to control the reactor vessel temperature or the approach-to-saturation temperature, that is, the difference between the flue-gas dry-bulb and wet-bulb temperatures.

Semidry systems inherently have lower parasitic energy requirements than wet FGD systems, for several reasons. Since the spent sorbent is dried by the energy in the flue gas, no costly dewatering equipment is required. Also, semidry systems have a lower slurry pumping requirement compared to their wet FGD system counterparts.

Circulating dry scrubbing

Circulating dry scrubbing (CDS) is a relatively new semidry FGD process that has been proposed to compete with spray-dryer systems. CDS incorporates dry sorbent recirculation to achieve high sulfur capture and sorbent utilization under typical spray-drying operating conditions. A simplified CDS system is illustrated in Figure 1. Slurry composed of hydrated lime and dilution water is injected into the bottom of a reaction chamber cocurrently with flue gas. The flue gas suspends, dries, and transports the sorbent through the reaction vessel and out into a cyclone-type particulate collector. A large portion of both the spent and unutilized sorbent collected in the cyclone is reinjected into the reactor vessel as a dry powder. This recycle improves the utilization of the calcium-based sorbent and provides a reaction substrate for the incoming hydrated lime slurry. In comparison to conventional spray-dryer systems, where recycled solids are slurried and atomized with the fresh sorbent, very high recycle ratios are possible in a CDS process where only dry solids are recycled. A portion of the captured cyclone solids is removed from the system to prevent excessive accumulation of solids within the reactor vessel.

Although there are a few full-scale CDS applications (Graf, 1985; Toher et al., 1991), very little data exists on the operation of these units or on the fundamental chemistry and mechanisms of SO_2 removal. Indeed, there are many similarities between spray-dryer and CDS technologies; however, the higher surface area available in a CDS reactor may influence both evaporation and absorption rates, and diffusion limitations. Therefore, the objectives of this research were to: determine the effect of variable solids concentration in the reactor on sulfur capture; elucidate the reaction mechanisms through analysis of the chemical composition and morphology of the spent sorbent particles; and develop a simple mathematical model to describe the three-phase reaction system of the CDS process.

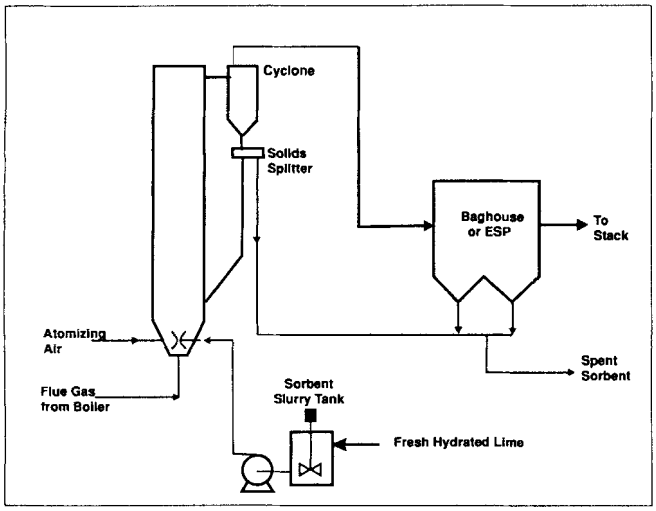

Figure 1. Typical circulating dry scrubber process.

Background of Previous Semidry FGD Models

Spray-Drying absorption reaction chemistry and process considerations

Once the sorbent slurry is contacted with the SO_2-laden flue gas, several reaction steps are thought to occur concurrently with evaporation (Keener et al., 1989):

Overall Reaction:

$$Ca(OH)_2 + SO_2 = CaSO_3 \cdot 1/2H_2O + 1/2H_2O.$$

1. Diffusion of SO_2 from the bulk gas to the droplet surface.
2. Absorption of SO_2 at the droplet surface:

$$SO_2(g) = SO_2(aq).$$

3. Interception of dry sorbent particles into the droplet.
4. Dissolution of SO_2 to from HSO_3^- and SO_3^{2-}:

$$SO_2(aq) + H_2O(l) = H^+(aq) + HSO_3^-(aq)$$

$$HSO_3^-(aq) = H^+(aq) + SO_3^{2-}(aq).$$

5. Diffusion of liquid phase sulfur species within the droplet.
6. Dissolution of $Ca(OH)_2$ particle:

$$Ca(OH)_2(s) = Ca^{2+} + 2OH^-.$$

7. Precipitation of calcium sulfite:

$$Ca^{2+} + SO_3^{2-} + 1/2H_2O(l) = CaSO_3 \cdot 1/2H_2O(s).$$

The reactivity of the slurry droplets toward SO_2 is a strong function of how long the bulk water phase is maintained. Since these reactions occur in the aqueous phase, the removal of water by evaporation severely limits reaction steps 2, 4, 5, and 6. The reactivity of the slurry is also dependent upon the droplet size. Although smaller drops have a higher surface area than large drops and thus allow higher SO_2 absorption rates, their water also evaporates faster, so their effective "wet lifetime" is decreased. Thus, it seems logical that the larger drops, having a longer wet lifetime, would be more reactive. However, it has been shown (Newton et al., 1990) that an optimum diameter exists due to the gas mass-transfer limitations of larger drops that can be attributed to the smaller surface area per volume ratio.

Spray-drying evaporation stages

The slurry droplet moisture content vs. time profile, shown in Figure 2, is thought to be similar to that calculated from classic spray-drying theory (Cole et al., 1990). Depending on the atomization method, slurry droplet diameters can range from 20 to 150 μm. Suspended inside each droplet are hundreds of $Ca(OH)_2$ particles ranging from 1 to 5 μm in diame-

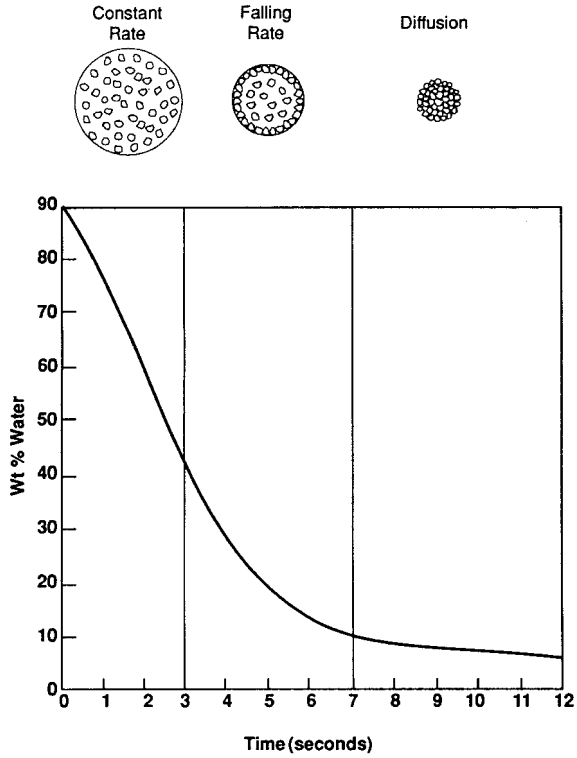

Figure 2. Spray drying absorption particle reaction stages.

ter. These sorbent particles begin to dissolve to the extent that they saturate the water in the droplet. At the same time, SO_2 is absorbed on the droplet surface.

As slurry droplets pass through the reactor or duct, water begins to evaporate rapidly and the sorbent particles inside the droplets become more concentrated (this is known in the literature as the *constant rate period*). During this initial drying period, evaporation of water takes place from the free droplet surface. After about 3 s, the sorbent particles inside the droplet accumulate preferentially at the surface to form a solid barrier, thus limiting the evaporation and sulfur capture rates (hence, this is called the *falling rate period*). After approximately seven seconds, most of the free water phase within the solid agglomerate is removed by evaporation.

Usually, the inner core of the spray-dryer agglomerate contains unreacted $Ca(OH)_2$, a consequence of the rate of water evaporation exceeding the rate of SO_2 absorption. Once the moisture content of the agglomerate has reached equilibrium, the SO_2 absorption rate becomes very low. At spray-drying operating conditions (54 to 77°C or 130 to 170°F), the reaction rate of dry $Ca(OH)_2$ with gaseous SO_2 is kinetically limited.

After approximately 10 s, the moisture content of the spent sorbent particles has been lowered to 3 to 5 wt. % and the flue gas exits the spray-dryer absorber. The particles are then collected in either an electrostatic precipitator (ESP) or a fabric filter baghouse. Here, the reactivity of the spent sorbent particles toward SO_2 in the flue gas is low due to their low moisture content. Nevertheless, an additional 10 to 20% sulfur capture can be observed where a filter is used, due to the flow across the filter cake of the particulate control device.

Proposed CDS Model

The reaction chemistry for a CDS process is thought to be very similar to that in the spray-drying process described in the previous section. The major differences between the two systems are primarily the increased solids concentration within the CDS reactor vessel and the method for injecting the recycle solids. Efficient sorbent atomization is not as crucial for the CDS configuration because the slurry is scavenged by, and spread over, the recycle solids. The entrained solids in the CDS reactor provide increased surface area for SO_2 absorption. In addition, the turbulent nature of the fluid bed in the CDS system decreases the gas-side resistance of SO_2 to the reactive solid surfaces.

Reactor solid particle growth

In a CDS reactor, the ratio of solids-to-water is several orders of magnitude greater than that found in a conventional spray-drying process. In a slurry droplet, $Ca(OH)_2$ particles are suspended in a spherical water droplet. With CDS processes, the slurry is dispersed over spherical solid particles, as shown in Figure 3a. A nozzle in the bottom of the fluid bed atomizes the slurry into droplets ranging from 20 to 100 μm in diameter. Recycled solid particles, ranging in di-

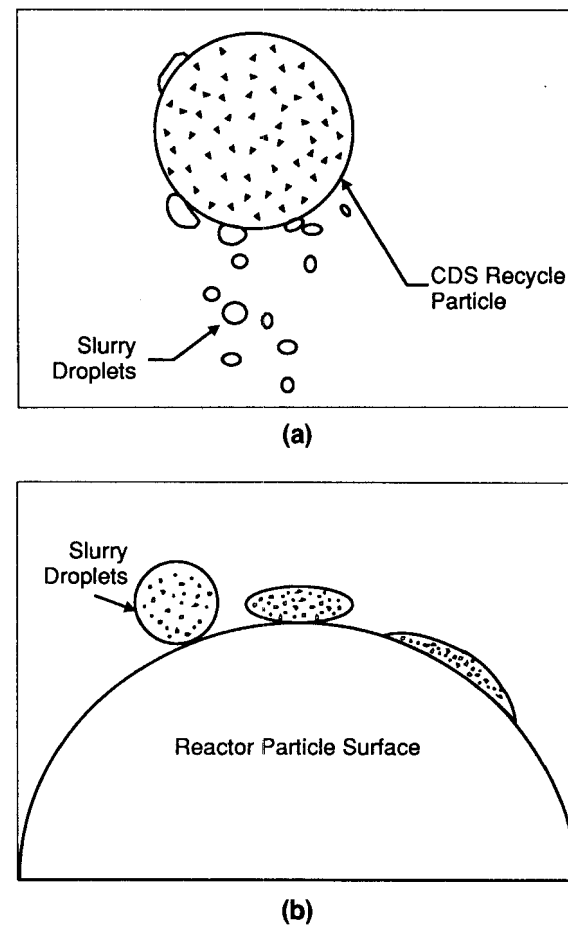

Figure 3. (a) Recycle particles capturing sorbent slurry; (b) possible scenarios for slurry coverage on recycle particles.

ameter from 20 to 200 μm, capture all or a portion of these droplets by combination of inertial impaction and interception.

If the slurry were to completely cover every sorbent particle equally, the thickness of the slurry layer would range from approximately 0.1 to 0.6 μm, depending on the volumetric rate of humidification water (such as the approach-to-saturation temperature varying from 0° to 5°C) and the recycle ratio of solids (such as with reactor solids concentration varying from 6,000 to 12,000 $g \cdot m^{-3}$). The fractional coverage of the slurry over the solid particles depends upon several factors: surface tension of the slurry; the hydrophilicity of the solid particles; the evaporation rate of the water contained in the slurry; and the diameter of the droplet and the recycle particle. Several possible scenarios of slurry coverage on the reactor particle surface are illustrated in Figure 3b.

As the wetted area of each particle begins to evaporate, SO_2 is absorbed and reacts with the dissolved $Ca(OH)_2$ to form $CaSO_3$. Since $CaSO_3$ is relatively insoluble under these conditions, fine crystals will precipitate in solution. When the slurry completely evaporates, the $CaSO_3$ product will deposit onto the recycled particles. Most of these particles will be recycled many times over; each time through the process they will accumulate a layer of $CaSO_3$ reaction product and unreacted sorbent on their outer surfaces.

This growth phenomenon can continue until the diameter of the particle is such that the superficial velocity in the reactor is no longer above its terminal velocity, which at this point, the particle could drop out of the reactor. Alternatively, particle growth could be interrupted by breakup of the surface or attrition. If more particles drop out than are attrited, new particles must be formed to maintain a steady-state mass balance of solids in the reactor. These new particles could form from smaller "seed" particles such as fly ash or spray-dryer-like agglomerates of sorbent and reaction products. Therefore, it is possible that each reactor particle will consist of many distinct layers from each pass through the reactor. Thus, the outer structure of the CDS reactor particles may resemble that of an onion while the core could consist of a seed particle(s) as shown in Figure 4.

Inherently, the nature of a fluid-bed system is turbulent and therefore chaotic. Complete simulation of the flow physics and reaction kinetics was beyond the scope of this experimental study. Several simplifying assumptions were made for the development of a mathematical model:

1. Gas and particle flow inside the reactor vessel are considered to be plug flow.
2. The reactor solids are equally distributed throughout the reactor. Since the void volume is very high, the bubble phase will be neglected.
3. Reactor particle attrition is negligible.
4. The particle-size distribution can be described by the mean particle size.
5. Water evaporation is adiabatic and is limited by diffusion only.
6. Mass transfer of SO_2 is limited by liquid phase diffusion. The gas-phase resistance term is negligible.
7. The reaction of the dissolved calcium hydroxide and SO_2 is instantaneous.
8. All of the atomized slurry droplets are scavenged by the recycled reactor particles.

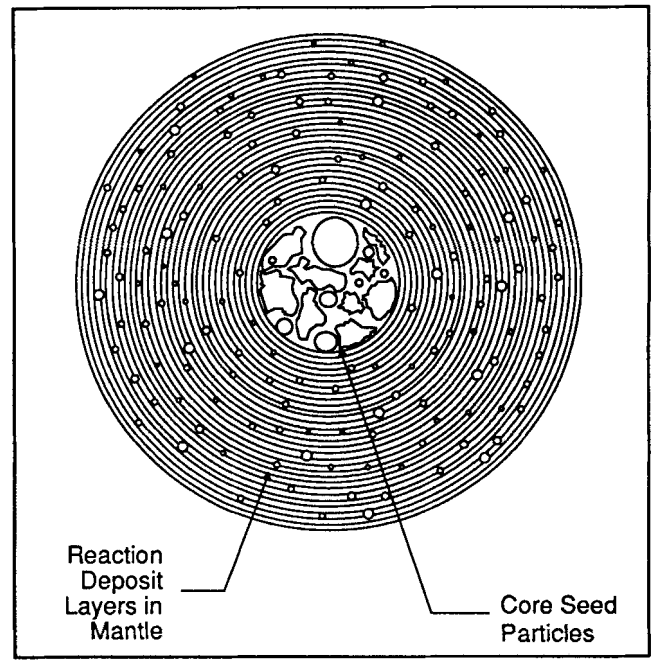

Figure 4. Theoretical circulating dry scrubber particle morphology.

9. The FGD reactions occur only in the water phase. Once the water phase evaporates, the sorbent reactivity is negligible.
10. The reaction products (namely calcium sulfite) deposit on and adhere to the reactor recycle particles.
11. Although carbonation of $Ca(OH)_2$ can be substantial in industrial FGD processes, it was ignored since the concentration of CO_2 in the synthetic flue gas used for this was relatively low (less than 3.0%).

Mass flux equation of SO_2 to the wetted surface area

The reaction kinetics in the liquid phase have been shown to be much faster than the diffusion times of sorbent and dissolved sulfur species (Babu et al., 1984). Therefore, the reaction of the dissolved sulfur species with the sorbent can be considered instantaneous for the purpose of model development. A reaction front with the liquid phase will exist where the concentration of both the dissolved sorbent and sulfur species are zero.

Notation for the following equations are presented at the end of this manuscript. The flux from the gas phase onto the liquid surface can be expressed in terms of the mass-transfer coefficient:

$$N_A = \frac{k_g}{RT}(P_A - P_{Ai}). \tag{1}$$

The interfacial partial pressure of A, P_{ai}, can be expressed in term of Henry's law constant and the liquid phase concentration of dissolved H_2SO_3:

$$P_{Ai} = HC_{Ai}. \tag{2}$$

The flux can also be expressed in terms of the liquid phase parameters as

$$N_A = \Phi k_{Al} C_{Ai}, \tag{3}$$

where

$$\Phi = \left(\frac{D_{Bl}}{D_{Al}} \frac{C_{Bs}}{C_{Ai}} + 1 \right),$$

The parameter Φ is the enhancement factor to account for chemical reaction and the dissolution of SO_2.

By combining Eqs. 1, 2 and 3, we can eliminate the unknown variable, C_{Ai}. Therefore, we can obtain the SO_2 flux equation for the active wetted surface area of the slurry on the reactor particles:

$$N_A = \frac{(P_A/H) + \beta C_{Bs}}{(RT/k_g H) + \dfrac{1}{k_l}}, \tag{4}$$

where $\beta = D_{Bl}/D_{Al}$. Equation 4 can also be written in terms of the enhancement factor, Φ, and the overall mass-transfer coefficient, K_G, as shown in Eq. 5.

$$N_A = \frac{P_A}{(RT/k_g) + (H/\Phi k_l)} = K_G P_A. \tag{5}$$

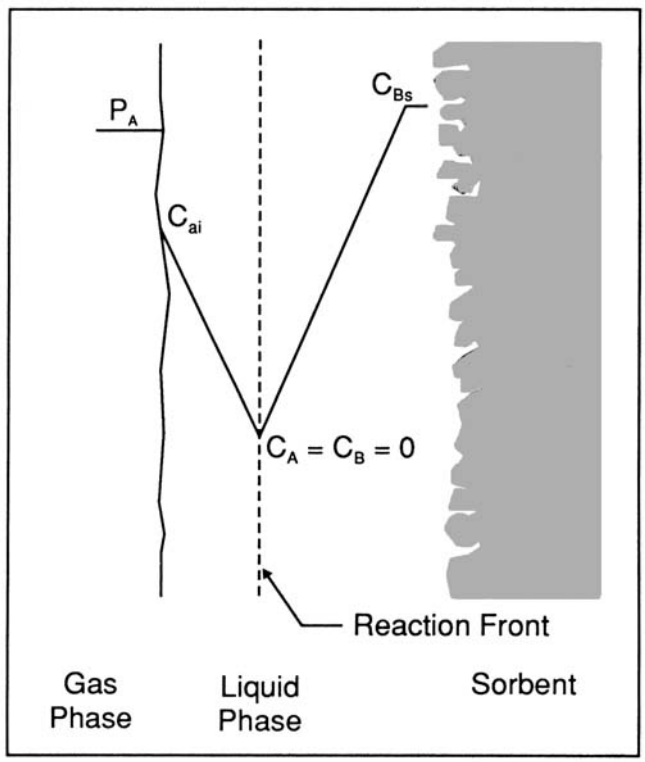

Figure 5. Concentration profile for diffusing lime and sulfur species.

Mass-transfer resistances described by Eq. 5 and a hypothetical concentration profile for the diffusing lime and sulfur species are shown in Figure 5.

Global SO_2 mass transfer

A mole balance of SO_2 within the reactor vessel yields the following differential equation:

$$\frac{\upsilon \rho_m}{P} \frac{dP_A}{dz} = -N_A a. \tag{6}$$

By multiplying through by $dz/(N_A \upsilon)$ we obtain

$$\frac{\rho_m}{P} \frac{dP_A}{N_A} = -\frac{dz}{\upsilon} a = -a dt. \tag{7}$$

Substituting Eq. 5 into Eq. 7 gives

$$\frac{\rho_m}{P} \frac{dP_A}{K_G P_A} = -a dt, \tag{8}$$

where K_g, the overall mass-transfer coefficient, is defined as

$$\frac{1}{K_g} = \frac{RT}{k_g} + \frac{H}{\Phi k_l}. \tag{9}$$

If the gas-side resistance in the fluid bed is negligible, then k_g is much larger than k_l, and Eq. 9 can be simplified to the following:

$$K_G = \Phi \frac{k_l}{H}. \tag{10}$$

The enhancement factor to account for dissociation of SO_2 in water, neglecting gas-side resistance (Froment and Bischoff, 1990), that is, $P_{Ai} = P_A$, is

$$\Phi = 1 + \beta H \frac{C_{BS}}{P_A}. \tag{11}$$

Substitution of Eqs. 9, 10, and 11 into Eq. 8 and subsequent integration of the differential equation yields:

$$\int_{P_{A_{in}}}^{P_{A_{out}}} \frac{dP_A}{(P_A k_l/H) + \beta C_{Bs} k_l} = -\int_0^t \frac{aP}{\rho_m} dt. \tag{12}$$

The RHS upper boundary condition for Eq. 12, t, is the effective mass-transfer time of the slurry liquid phase; t is likely to be much less than the gas residence in the reactor (if drying is nearly complete).

Upon integration and rearrangement of Eq. 12, we can obtain an expression for the fraction of SO_2 captured:

$$E_{SO_2} = 1 - \frac{P_{A_{out}}}{P_{A_{in}}} = \left(1 + \frac{\beta H C_{Bs}}{P_{A_{in}}} \right) (1 - e^{(-k_l a P/H \rho_M) t}). \tag{13}$$

The value of E_{SO_2} cannot be calculated at this point because k_l, a, and t are unknowns in the RHS of Eq. 13.

Water evaporation

Since the absorption of SO_2 is considered primarily an aqueous reaction, the evaporation rate of the liquid phase is important for determining the overall sulfur capture in a CDS system. The water flux equations used for the spray-drying constant rate drying period for droplet evaporation may be used for CDS analysis. However, the determination of the surface area for evaporation is more complicated in a CDS system. It is unlikely the total reactor particle surface area in the reactor vessel at any particular time is available for evaporation. Most likely, only a portion of the solids are covered with the slurry. Also, some slurry droplets may avoid contact with reactor particles.

Assuming plug flow and neglecting axial diffusion of water vapor, a differential mole balance along the reactor yields the following differential equation:

$$\frac{\upsilon \rho_M}{P}\frac{dP_w}{dz} = F_w a, \tag{14}$$

where
F_w = flux of H_2O from the liquid surface
a = area of liquid surface per volume of gas

The water evaporation flux can be estimated from the following equation, which accounts for both convection and molecular diffusion (Kinzey, 1988):

$$F_w = k_w \rho_M \ln\left(\frac{P - P_w}{P - P_{\text{sat}}}\right). \tag{15}$$

By multiplying Eq. 14 by dz/υ, the following equation can be obtained:

$$\frac{dP_w}{F_w} = \frac{aP}{\rho_M}\frac{dz}{\upsilon} = \frac{aP}{\rho_M}dt. \tag{16}$$

Upon substitution of Eq. 14 into Eq. 15 and integration of the resulting equation, the following is obtained:

$$\int_{P_{w,\text{in}}}^{P_{w,\text{out}}} \frac{dP_w}{\ln\left(\frac{P - P_w}{P - P_{\text{sat}}}\right)} = \int_0^{t_{\text{evap}}} k_w a P dt. \tag{17}$$

By solving for the evaporation time, t_{evap}, in Eq. 17, we have:

$$t_{\text{evap}} = \frac{1}{k_w a P}\int_{P_{w,\text{in}}}^{P_{w,\text{out}}} \frac{dP_w}{\ln\left(\frac{P - P_w}{P - P_{\text{sat}}}\right)}. \tag{18}$$

The gas-side mass-transfer coefficient, k_w, can be estimated from the Ranz and Marshall correlation (Ranz and Marshall, 1952). Unfortunately, the evaporation time cannot be calculated directly with Eq. 18 since the specific surface area or coverage of the liquid slurry, a, is unknown.

Overall sulfur capture equation

In the previous section, expressions for the evaporation time and the fraction of SO_2 captured were derived. However, four unknown variables remain: (1) the specific surface area, a; (2) the liquid phase mass-transfer coefficient, k_l; (3) the mass-transfer time, t, and; (4) the evaporation time, t_{evap}. The unknown mass transfer time can be estimated by assuming that SO_2 absorption/reaction occurs only when a liquid phase is present; so $t_{\text{evap}} = t$. Also, t, a, and P can be eliminated by combining Eq. 18 and Eq. 13 to yield

$$E_{SO_2} = \Phi_0\left[1 - \exp\left(\frac{-k_l}{H\rho_M}\frac{1}{k_w}\int_{P_{w,\text{in}}}^{P_{w,\text{out}}} \frac{dP_w}{\ln\left(\frac{P - P_w}{P - P_{\text{sat}}}\right)}\right)\right], \tag{19}$$

where Φ_0 is the initial enhancement factor and is given as

$$\Phi_0 = \left(1 + \frac{\beta H C_{Bs}}{P_{A_{\text{in}}}}\right).$$

An important feature of Eq. 19 is that the fraction of SO_2 *captured is independent of the specific wetted surface area in the reactor.* At first glance this may seem counterintuitive. However, it is reasonable because of the two competing mass transfer processes taking place concurrently: water evaporation and SO_2 absorption into the water phase. For example, if the specific surface area of a given volume slurry is increased, then the absorption rate of SO_2 increases. Additional surface area also increases the water evaporation rate so the SO_2 capture remains unchanged. This phenomenon has been verified experimentally by Neathery (1993); several short tests were conducted to gauge the effect of the solids recycle rate or solids concentration on SO_2 capture. The differential pressure across the reactor length was found to be a good indicator of the concentration of flowing solids inside the reactor vessel. During the parametric test program, the concentration of flowing recycle solids varied between 5,750 and 11,500 g/m^3, which corresponds to a reactor differential pressure of approximately 50 to 100 Pa, respectively. This variation did not have any measurable effect on the reactor sulfur capture.

The only unknown variable in Eq. 19 is the liquid-side mass-transfer coefficient, k_l. This coefficient is defined as

$$k_l = \frac{D_{Al}}{\delta}, \tag{20}$$

where δ is the diffusion distance or film thickness in the liquid phase. In conventional spray-drying theory, δ can be estimated to be some fraction of the sorbent particle diameter (for example, $\delta = d_p/2$, as used by Dantuluri et al., 1991). This estimation is based on film theory for spherical particles suspended in an infinite medium. For spray-drying conditions, where sorbent particles are suspended in large water droplets, this may be a valid assumption. For CDS, this assumption is not reasonable because the diameter of the fresh $Ca(OH)_2$ particles are much larger than the scale of the wa-

ter layer thickness (δ). The reactor sulfur capture was found to be a function of known or easily estimated parameters, with the exception of the liquid-phase mass-transfer coefficient, k_l (Eq. 19). This parameter is usually estimated as the liquid-phase diffusivity divided by the diffusion distance, δ. However, for the current application, this distance is very difficult to approximate because of the relatively thin film thicknesses around the solid $Ca(OH)_2$ particles in the slurry. The parameter δ is related to the interparticle spacing of the sorbent and depends on the ratio of water-to-$Ca(OH)_2$ in the sorbent slurry; therefore, k_l should be a function of the approach-to-saturation temperature and Ca/S ratio.

To judge the validity of the proposed model, it would be useful to solve for a reference mass transfer parameter that is independent of the Ca/S ratio or the approach-to-saturation temperature. Therefore, the effective mass-transfer coefficient calculated was estimated by the following equation:

$$k_l(\text{Ca/S, ASAT}) \approx k_{l(\text{ref})}\left(\frac{w(\text{Ca/S, ASAT})}{w_{\text{ref}}}\right), \qquad (21)$$

where

Ca/S = inlet molar ratio of calcium to sulfur
ASAT = approach-to-saturation temperature
w = weight percent solids in the initial slurry mixture
w_{ref} = weight percent solids at the reference conditions
$k_{l(\text{ref})}$ = mass transfer coefficient at the reference conditions

A convenient reference condition can be defined with a Ca/S feed ratio of unity at saturated conditions (ASAT = 0). The water content of the slurry at this reference would correspond to the maximum dilution of sorbent particles, which therefore define the maximum interparticle spacing and the minimum k_l. Thus, $k_{l(\text{ref})}$ and w_{ref} are constants that can be calculated and w is only a function of the Ca/S ratio and the approach-to-saturation temperature. So if the approach-to-saturation is increased above zero (lowering the ratio of water-to-sorbent in the slurry), the fraction of solids, w, will increase, and thus the mass transfer coefficient will increase proportionally due to the decrease in δ. Likewise, as the Ca/S ratio is increased above unity, the sorbent solids fraction increases, and k_l will increase proportionally. Substitution of Eq. 21 into Eq. 19 yields the following equation:

$$E_{SO_2} = \Phi_0\left[1-\exp\left(\frac{-k_{l_{\text{ref}}}\left(\frac{w}{w_{\text{ref}}}\right)}{H\rho_M}\frac{1}{k_w}\int_{P_{w,\text{in}}}^{P_{w,\text{out}}}\frac{dP_w}{\ln\left(\frac{P-P_w}{P-P_{\text{sat}}}\right)}\right)\right]. \qquad (22)$$

Here, the reference mass-transfer parameter $k_{l(\text{ref})}$ is still unknown; however, it is independent of the Ca/S ratio and the approach-to-saturation temperature. A FORTRAN computer code, called CBAFGD (Circulating Bed Absorption for Flue-Gas Desulfurization), was developed to solve for $k_{l(\text{ref})}$ using the pilot-plant data from selected experimental data groupings. The solution of Eq. 2 requires the estimation of several physical properties of the gas and liquid phases. All of these parameters were estimated from correlations based on theory and/or experimental data (Cole et al., 1990; Ranz and Marshall, 1952); a complete description of these correlations has been given (Neathery, 1993).

Results and Discussion

All of the experimental data utilized for this study were obtained from a 0.308-m (12-in.)-diameter CDS reactor system; a detailed description of the apparatus and experimental procedure has been given in a previous study (Neathery, 1993). Calcium chloride ($CaCl_2$) was added to the sorbent slurry in sufficient quantity to simulate a 0.20 to 0.25% Cl content coal. Baseline tests without Cl addition were also performed.

The presence of fly ash could also be beneficial with respect to particle nucleation and subsequent agglomeration of individual particles. As the CDS reactor particles grow to the point where they drop out of the fluidized bed, new particles must be formed to replace the surface area. Fly ash from the incoming flue gas could help to "seed" the formation of new CDS particles. To study this possibility, low chlorine content fly ash from a local utility boiler was injected into the synthetic flue gas upstream of the CDS reactor during selected experiments. The fly ash originated from a mixture of eastern bituminous coal and was found to have a relatively small available alkalinity (less than 2 wt. % as CaO, Neathery, 1993). Fly ash was injected into the flue gas at a rate to maintain an effective concentration ranging from 0.0 to 2.9 g/m^3 (0 to 2.5 gr/ACF). During the selected tests with fly ash injection, the slight contribution of the fly ash alkalinity was compensated by adjusting the effective inlet Ca/S; hence, the chemical effects due to the fly ash were negated.

Other important independent variables such as Ca/S ratio, approach-to-saturation temperature, and inlet flue-gas temperature were included in the basic experimental matrix so that qualitative comparisons could be obtained between the spray-drying and CDS systems. Measured sulfur capture values and the respective process parameters from a series of experiments were applied to the CBAFGD model. The data were analyzed in five separate groups: (1) 1,700 ppm inlet SO_2, without ash injection and without $CaCl_2$; (2) 1,700 ppm inlet SO_2, with ash injection, and without $CaCl_2$; (3) 2,500 ppm inlet SO_2, with ash injection and without $CaCl_2$; (4) 1,700 ppm inlet SO_2, without ash injection and with $CaCl_2$; and (5) 1,700 ppm inlet SO_2, with ash injection and with $CaCl_2$.

In each of these data groupings, the reference liquid-phase mass transfer coefficient $k_{l(\text{ref})}$, was computed. Averages of the parameter $k_{l(\text{ref})}$ from each group were used to calculate the predicted fraction of SO_2 captured. Values of the predicted fraction of sulfur capture were plotted against the measured values to gauge the validity of the model.

Model comparison without chloride addition: (Groups 1, 2, and 3)

Comparisons of the predicted vs. measured sulfur capture values for the data groups without $CaCl_2$ are plotted in Figures 6, 7, and 8. Figure 6 shows the model's accuracy without fly ash injection and without $CaCl_2$ addition to the slurry

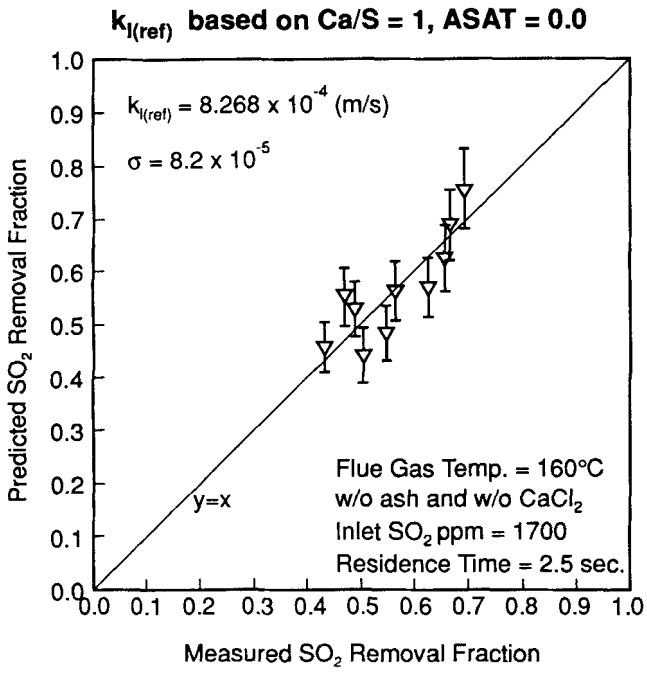

Figure 6. Predicted vs. experimental SO_2 capture.

Group 1 data: 1,700 ppm inlet SO_2, without ash injection and without $CaCl_2$.

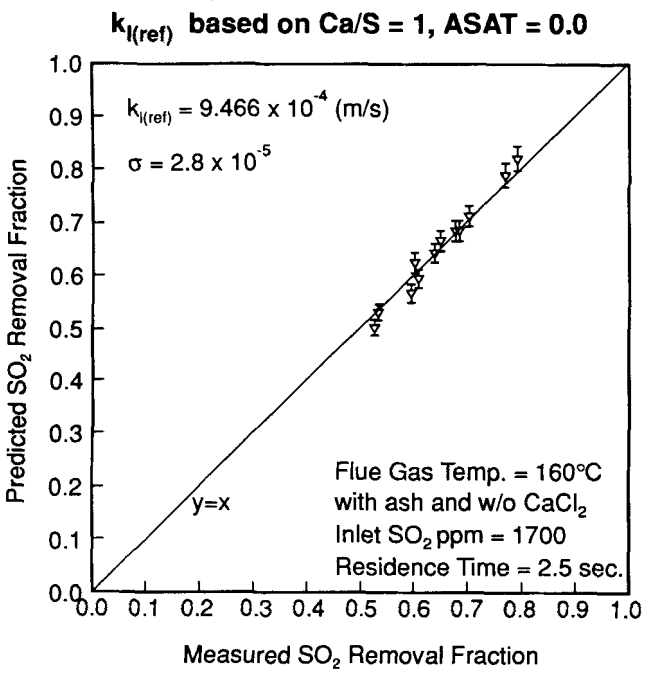

Figure 7. Predicted vs. experimental SO_2 capture.

Group 2 data: 1,700 ppm inlet SO_2, with ash injection and without $CaCl_2$.

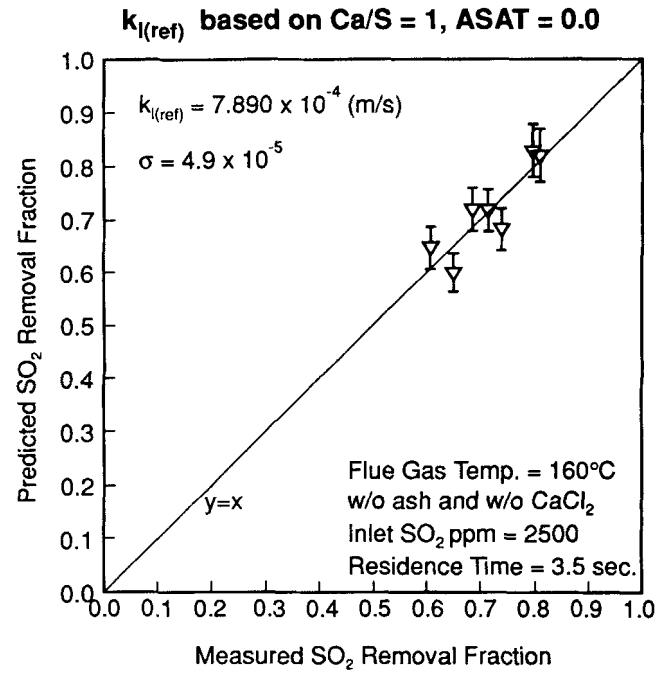

Figure 8. Predicted vs. experimental SO_2 capture.

Group 3 data: 2,500 ppm inlet SO_2, with ash injection and without $CaCl_2$.

(Group 1). The computed mean value of $k_{l(ref)}$ was 8.268 $\times 10^{-4}$ m/s with a standard deviation of $\pm 8.2 \times 10^{-5}$. The error bars show the variability of the predicted sulfur capture fraction due to the standard deviation of $k_{l(ref)}$. Here, the relative deviations in sulfur capture were approximately ± 5 percentage points. The relative errors for the predicted sulfur capture values ranged from -17.0% to 12.0% with an average relative error of 8.2%.

Shown in Figure 7 is the model comparison with fly ash injection and without $CaCl_2$ (Group 2). The mass-transfer parameter $k_{l(ref)}$ was calculated to be 9.466×10^{-4} m/s, which was nearly 15% higher than the case without fly ash injection in the Group 1 data. Here, the variability of the predicted sulfur capture was much lower than the first data group since the standard deviation of $k_{l(ref)}$ was only $\pm 2.8 \times 10^{-4}$ m/s; this resulted in an average variability of $\pm 2.5\%$ for the predicted sulfur capture. The relative errors for the predicted sulfur capture values ranged from -3.6 to 5.1% with an average relative error of 2.2%.

Figure 8 shows the model's accuracy for the higher SO_2 inlet concentration (2,500 ppm) with fly ash injection and without $CaCl_2$ addition to the slurry (i.e., Group 3). The parameter $k_{l(ref)}$ was calculated to be 7.890×10^{-4} m/s with a standard deviation of $\pm 4.9 \times 10^{-5}$ m/s. This was the lowest mass transfer parameter calculated for the data groups without $CaCl_2$ enhancement of the sorbent slurry: 5% lower than Group 1 and nearly 20% lower than Group 2. Relative errors of the predicted sulfur capture values ranged from -7.3 to 7.6% with an average relative error of 4.7%.

Of the data groups analyzed without $CaCl_2$ enhancement, the highest mass-transfer parameter was calculated with fly ash injection and with an inlet SO_2 concentration of 1,700 ppm. The lowest mass transfer parameter was calculated with fly ash injection at the 2,500 ppm SO_2 inlet concentration. Part of the decrease at the higher SO_2 level can be explained by the higher interfacial liquid concentration of H_2SO_3; at the higher SO_2 concentration, the dissociation of H_2SO_3 is lowered, thereby decreasing the liquid phase mass-transfer coefficient. The highest accuracy of the model was exhibited by the data groups with fly ash injection.

Mass-transfer coefficient estimation with $CaCl_2$ addition: Groups 4 and 5

The objective of the model development was to mathematically describe a simple CDS system without additive enhancements such as $CaCl_2$. With $CaCl_2$ added to the feed slurry, the vapor pressure of the water in the sorbent slurry is lowered and therefore retards the evaporation rate. As water is evaporated from the slurry, the $CaCl_2$ becomes more concentrated until its vapor pressure equals the bulk gas H_2O vapor pressure.

In the current model, the integral to compute the evaporation time, as shown in Eq. 18, would become infinite if vapor pressure modification from the $CaCl_2$ was considered; therefore, the assumption that $t_{evap} = t$ would not be valid here. To avoid this problem, the data groups with chloride enhancement were analyzed without considering the $CaCl_2$ content in the slurry; therefore, complete evaporation of the slurry was considered with the evaporation rate computed as with the pure sorbent slurry in Groups 1 to 3. Without considering the retarded evaporation rates, the value of $k_{l(ref)}$ was considered a pseudo-mass-transfer coefficient (this coefficient was denoted as $k'_{l(ref)}$) and was computed to qualitatively compare the effect of chloride in the feed slurry.

Figure 9 shows the graphical comparison of the predicted and measured sulfur capture for the test conditions without fly ash injection and with $CaCl_2$ addition (i.e., Group 4). The calculated pseudo-mass-transfer coefficient, $k'_{l(ref)}$ averaged 1.0248×10^{-3} m/s with a standard deviation of 3.34×10^{-5} m/s. The relative error for the predicted sulfur capture in Group 4 ranged from -5.1 to 4.3% with an average absolute relative error of 2.5%.

Figure 10 shows the graphical comparison of the predicted and measured sulfur capture for the test conditions with fly ash injection and with $CaCl_2$ enhancement of the sorbent

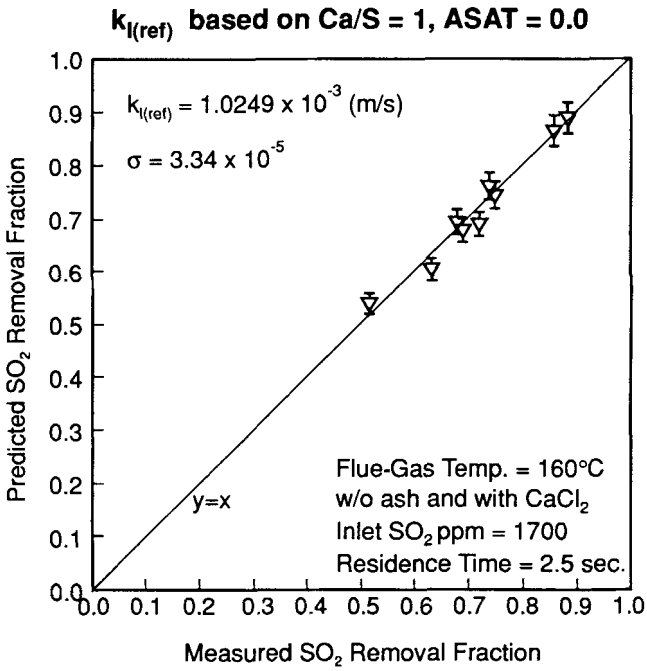

Figure 9. Predicted vs. experimental SO_2 capture.

Group 4 data: 1,700 ppm inlet SO_2, without ash injection and with $CaCl_2$.

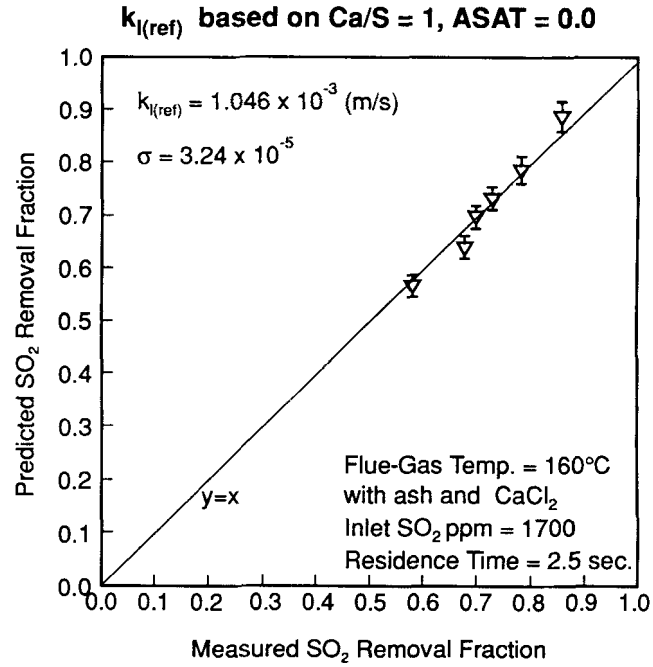

Figure 10. Predicted vs. experimental SO_2 capture.

Group 5 data: 1,700 ppm inlet SO_2, with ash injection and with $CaCl_2$.

slurry (i.e., Group 5). The calculated pseudo-mass-transfer coefficient, $k'_{l(ref)}$ averaged 1.046×10^{-3} m/s with a standard deviation of 3.24×10^{-5} m/s, and was quite similar to the Group 4 result. Relative errors of the predicted sulfur capture values in Group 5 ranged from -4.0 to 4.9% with an average absolute value relative error of 2.6%.

The effect of $CaCl_2$ enhancement can be realized by comparing the mass transfer parameters in Groups 2 to 5 and Groups 1 to 4 (the differences between these groups were the $CaCl_2$ enhancement). With $CaCl_2$, the increase in sulfur capture was 10.5% (from Group 2 to Group 5, with fly ash injection) and 24% (from Group 1 to Group 4, without fly ash injection).

Conclusions

This research has shown that the reaction chemistry of CDS is very similar to that of other semidry FGD processes such as spray-drying absorption, although many physical differences exist. The recycle ratio (rate of recycle: rate of sorbent feed) is much higher in a CDS reactor (1,000:1) as compared to that of spray-drying (4:1). As a result, a higher concentration of solid particulate exists in a CDS reactor, which can affect the mass transfer of both SO_2 absorption and water evaporation. CDS sulfur capture was found to be independent of the wetted surface area, a, since the falling rate and diffusion drying periods are insignificant, that is, no particle bunching occurs at the slurry/gas interface.

A mathematical model, CBAFGD, was developed to describe the chemical and physical mechanisms of CDS and to solve for the liquid-phase mass-transfer parameter, k_l. This parameter was modeled as a function of the sorbent-particle spacing on the recycle solids surface. A reference mass transfer coefficient was determined for conditions pertaining to a Ca/S ratio of unity and at saturation (i.e., ASAT = 0). Fly

ash in the flue gas was found to cause a small increase in $k_{l(\mathrm{ref})}$. Although the influence of chloride addition was not modeled in CBAFGD, a pseudo $k_{l(\mathrm{ref})}$ was also calculated based on the ideal conditions and was not affected by the presence of fly ash.

Acknowledgments

This work was supported by the University of Kentucky Center for Applied Energy Research (CAER) and the Tennessee Valley Authority (TVA). Discussions with Tom Burnett of the TVA and John Stencel of the CAER during the experimental work were greatly appreciated.

Notation

A = SO_2 component in the gas of liquid phases
B = dissolved $Ca(OH)_2$ in the liquid phase
C_A = concentrations of SO_2 in the liquid phase, kmol·m^{-3}
C_{Ai} = concentration of SO_2 at the gas–liquid interface, kmol·m^{-3}
C_B = concentration of dissolved lime in the liquid phase, kmol·m^{-3}
C_{Bs} = saturation concentration of $Ca(OH)_2$, kmol·m^{-3}
d_p = diameter of recycle particle, m
D_{Al} = diffusivity of dissolved SO_2 in the liquid phase, m^2·s^{-1}
d_{Bl} = diffusivity of dissolved $Ca(OH)_2$ in the liquid phase, m^2·s^{-1}
D_{wg} = diffusivity of water in the flue gas, m^2·s^{-1}
E_{SO_2} = fraction of SO_2 capture
H = Henry's law constant, atm kmol^{-1}·m^3
k_g = SO_2 mass transfer coefficient in the gas phase, m·s^{-1}
P = total gas pressure, atm
P_A = partial pressure of SO_2 in bulk gas, atm
$P_{A_{in}}$ = partial pressure of SO_2, reactor inlet, atm
$P_{A_{out}}$ = partial pressure of SO_2, reactor outlet, atm
P_w = partial pressure of H_2O, atm
P_{sat} = saturation pressure of H_2O, atm
R = ideal gas law constant, atm·m^3·kmol^{-1}·K^{-1}
T = gas temperature, K
T_{DB} = dry-bulb temperature, K
T_{WB} = wet-bulb temperature, K
v = superficial gas velocity, m·s^{-1}
z = axial reactor coordinate, m

Greek letters

ρ_m = molar density of the gas phase, kmol·m^{-3}
σ = standard deviation

Literature Cited

Babu, D. R., G. Narsimhan, and C. Phillips, "Absorption of Sulfur Dioxide in Calcium Hydroxide Solutions," *Ind. Eng. Chem. Fundam.*, **22**, 370 (1984).

Cole, J. A., G. H. Newton, J. C. Kramlich, and R. Payne, "Global Evaluation of Mass Transfer Effects: In-Duct Injection Flue Gas Desulfurization," Final Rep. U.S. Dept. of Energy, PETC Contract DE-AC22-88PC88873, Washington, DC (1990).

Dantuluri, S. R., W. T. Davis, R. M. Counce, and G. D. Reed, "Mathematical Model of Sulfur Dioxide Absorption Into a Calcium Hydroxide Slurry in a Spray Dryer," *Sep. Sci. Technol.*, **25**(13–15), 1843 (1991).

Froment, G. F., and K. B. Bischoff, *Chemical Reactor Analysis and Design*, 2nd ed., Wiley, New York (1990).

Graf, R., "First Operating Experience with a Dry Flue Gas Desulfurization (FGD) Process using a Circulating Fluid Bed (FGD-CFB)," *Circulating Fluidized Bed Technology*, P. Basu, ed., Pergamon Press, New York, p. 317 (1985).

Keener, T. C., S. J. Khang, J. R. Kadambi, R. J. Adler, M. E. Prudich, L. S. Fan, and K. Raghunathan, "Flue Gas Desulfurization for Acid Rain Control: A Critical Literature Review for Dry Calcium-based Sorbents and Processes," Report to the Ohio Coal Development Office, The Consortium of Ohio Universities, Cincinnati (1989).

Kinzey, M. K., Jr., "Modeling the Gas and Liquid-phase Resistances in the Dry Scrubbing Process for Sulfur Dioxide Removal," PhD Diss., Cornell Univ., Ithaca, NY (1988).

Kohl, A., and F. Riesenfeld, *Gas Purification*, Gulf Publishing, Houston (1985).

Neathery, J. K., "A Fundamental Study of Circulating Bed Absorption for Flue Gas Desulfurization," PhD Diss., Univ. of Kentucky, Lexington (1993).

Newton, G. H., J. Kramlich, and R. Payne, "Modeling the SO_2-Slurry Droplet Reaction," *AIChE J.*, **36**, 12 (1990).

Ranz, W. E., and W. R. Marshall, Jr., "Evaporation of Drops," *Chem. Eng. Prog.*, **48**(3), 141 (1952).

Toher, J. G., G. D. Lanois, and H. Sauer, "High Efficiency, Dry Flue Gas SO_x, and Combined SO_x/NO_x Removal Experience with the Lurgi Circulating Fluid Bed Dry Scrubber—A New, Economical Retrofit Option for U.S. Utilities for Acid Rain Remediation," SO_2 Control Symp., Washington, DC (1991).

Manuscript received Dec. 16, 1994, and revision received Feb. 24, 1995.